



Cite this: *Chem. Sci.*, 2021, **12**, 3264

All publication charges for this article have been paid for by the Royal Society of Chemistry

Received 12th September 2020
Accepted 28th December 2020

DOI: 10.1039/d0sc05071g
rsc.li/chemical-science

Introduction

Multicomponent molecular crystals,¹ such as salts and cocrystals, are highly valuable materials in pharmaceutical,^{2,3} medicinal⁴ and agrochemical^{5,6} research and development. They are also being investigated for applications in molecular electronics,⁷ energetic materials science^{8–10} and pigment chemistry.¹¹ Their functionality, and their significance to the management of patent life-cycles of specialty chemicals,^{12,13} has stimulated the development of various crystallisation and screening techniques for the rapid and thorough discovery of multicomponent molecular solids.¹⁴ Among those, mechanochemical tools¹⁵ emerged as particularly prominent as a result of their efficiency and accessibility.¹⁶

The mechanochemical preparation of salts and cocrystals—whether performed manually using a mortar and pestle, or automatically using mixer mills—is usually conducted in the presence of catalytic amounts of liquid additives to facilitate nucleation,¹⁷ to increase crystallisation rates,¹⁸ to enhance the crystallinity¹⁹ of the solid and to control polymorphism.²⁰ In

some cases, a mechanochemical reaction will not occur in the absence of such additives.^{21,22} The well-known benefits of using catalytic amounts of liquids in mechanochemical reactions, and the dearth of published reports (or even anecdotal evidence) demonstrating any detrimental effects of liquids, generally eliminates the inclination to knead materials in the absence of such additives.¹⁶ Only a small number of published reports mention such detrimental effects, and there is a pronounced shortage of comprehensive studies investigating instances wherein liquid additives have failed to facilitate cocrystal formation. The inability to mechanochemically form a multi-component crystal in the presence of a liquid additive has been, so far, associated with different phenomena. Studies by Friščić *et al.* and Shan *et al.* have attributed failed cocrystallisation attempts to the poor solubility of the cocrystal components in the liquid additive.^{17,18} A more recent study by Tumanov *et al.*, on the other hand, demonstrated that the absorption of atmospheric water by hygroscopic solids leads to the formation of viscous reaction mixtures wherein the reactant particles aggregate, thereby terminating the mechanochemical reaction.²³

Here, we describe instances wherein liquid additives unexpectedly inhibit, prohibit or reverse mechanochemical reactions. We suggest that the described inhibition and prohibition cannot merely be attributed to the poor solubility of the cocrystal components, or to the hygroscopicity and the viscosity of the reactants, but occurs through a mechanism different to those that have been earlier proposed.^{17,18,23} Our findings not only emphasise the multiplicity of roles that liquid additives can have in liquid-assisted grinding (LAG) processes, but also highlight the urgent need to adjust current protocols for highly popular liquid-assisted mechanochemical crystal-form screens, which are nowadays routinely performed in both academic and industrial settings.

^aFaculty of Chemistry, University of Warsaw, 1 Pasteura Street, Warsaw 02-093, Poland

^bDepartment of Chemistry, University College London, 20 Gordon Street, London WC1H 0AJ, UK. E-mail: d.bucar@ucl.ac.uk

^cDepartment of Chemistry and NIS Centre, University of Turin, Via Giuria 7, Torino 10125, Italy

^dDepartment of Chemistry, University of Cambridge, Lensfield Road, Cambridge CB2 1EW, UK

^eDepartment of Chemical and Pharmaceutical Sciences, University of Trieste, Piazzale Europa 1, 34127 Trieste, Italy. E-mail: dhasa@units.it

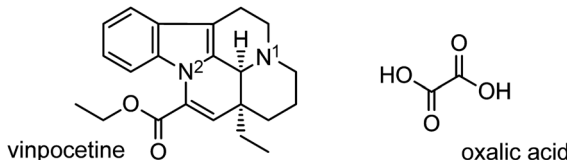
† Electronic supplementary information (ESI) available: Experimental methods, sample characterization, PXRD data, thermal analyses and DFT calculations. CCDC 2024365–2024367. For ESI and crystallographic data in CIF or other electronic format see DOI: 10.1039/d0sc05071g



Our interest in vinpocetine²⁴ (**vin**, Scheme 1)—a synthetic vincamine derivative used in the management of cerebrovascular conditions²⁵—inspired an extensive mechanochemical salt screen of **vin** involving a range of carboxylic acids and led to the discovery of a **vin** hydrogenoxalate salt, $(\text{Hvin}^+) \cdot (\text{Hoxa}^-)$. The reactants, **vin** and oxalic acid (H_2oxa , Scheme 1), were expected to form such a salt owing to their pK_a values, which exhibit a ΔpK_a value of approximately 6.5; a value that is significantly higher than the suggested threshold for salt formation.^{26,27} We subsequently performed a polymorph screen of this salt, the main aims of which were: (1) to elucidate the role of solvent polarity and its chemical nature (protic vs. aprotic) on the polymorphism of the $(\text{Hvin}^+) \cdot (\text{Hoxa}^-)$ salt, and (2) to determine how various quantities of the liquid additive affect the polymorphic outcome of the mechanochemical reaction. The second aim was prompted by the recent discovery of the fact that both the nature and amount of the liquid used in LAG reactions (defined by the η parameter¹⁷) can significantly affect the polymorphism of a mechanochemically prepared crystal form.²⁸ Other experimental parameters, such as milling frequency or the amounts of the starting materials used, were not varied in any of the performed LAG experiments reported here. Our results revealed the unusual inhibiting and prohibiting action of liquid additives in LAG crystal-from screens.

Results and discussions

Neat grinding of **vin** and H_2oxa for 60 min (in the absence of any liquid additives, $\eta = 0 \mu\text{L mg}^{-1}$) yielded an amorphous salt (Fig. 1). The formation of this salt was established using powder X-ray diffraction, and both ^{13}C and ^{15}N CPMAS solid-state NMR spectroscopy. In particular, it was observed that the signal at 29.3 ppm, corresponding to the N^1 atom in crystalline **vin** (Scheme 1), shifted downfield to 44.8 ppm in the spectrum of the amorphous solid (Fig. 2). This signal shift is consistent with those previously reported for **vin** salts²⁴ and for other solids containing protonated aliphatic nitrogen atoms.²⁹ We further showed that a crystalline salt does not form even when small amounts of liquid additives are used ($\eta = 0.05 \mu\text{L mg}^{-1}$). The formation of amorphous and poorly crystalline solids in LAG experiments is well known in cases where small amounts of liquid additives are used, and is often attributed to the evaporation of the volatile liquid additives before or during the milling process. We note, however, that this is not the case here, since liquids that exhibit low vapour pressures, namely dimethyl sulfoxide and 2-pyrrolidone, also yielded amorphous solids at $\eta = 0.05 \mu\text{L mg}^{-1}$.



Scheme 1 Molecular structures of vinpocetine (**vin**) and oxalic acid (H_2oxa), the constituents of the vinpocetine hydrogenoxalate salt. The two basic **vin** sites are highlighted as N^1 and N^2 .

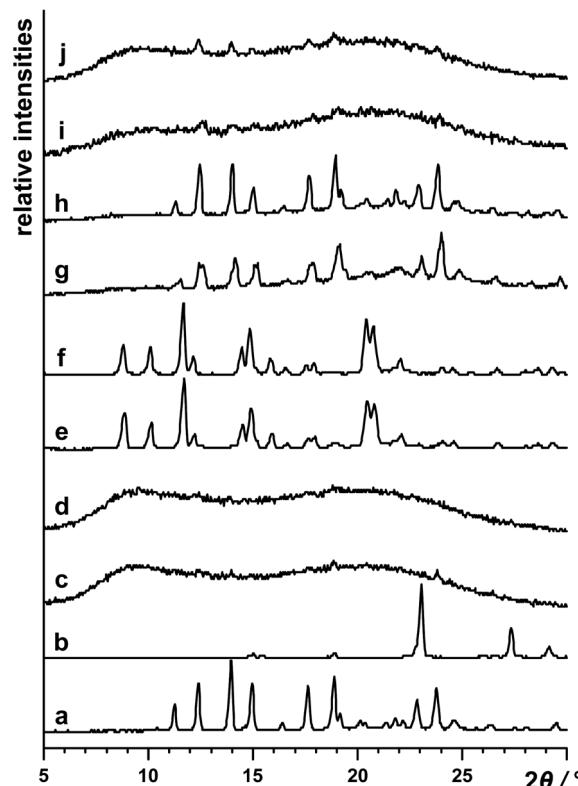


Fig. 1 Powder X-ray patterns of: (a) **vin**, (b) H_2oxa and (c) the product obtained by neat grinding for 60 min of **vin** and H_2oxa ($\eta = 0 \mu\text{L mg}^{-1}$). Diffractograms of products obtained via LAG of **vin** and H_2oxa , using various amounts of different liquid additives, are shown in: (d) ethyl acetate at $\eta = 0.05 \mu\text{L mg}^{-1}$, (e) ethyl acetate at $\eta = 0.15 \mu\text{L mg}^{-1}$, (f) ethyl acetate at $\eta = 0.30 \mu\text{L mg}^{-1}$, (g) nitromethane at $\eta = 0.15 \mu\text{L mg}^{-1}$, (h) nitromethane at $\eta = 0.30 \mu\text{L mg}^{-1}$, (i) ethanol at $\eta = 0.15 \mu\text{L mg}^{-1}$ and (j) ethanol at $\eta = 0.30 \mu\text{L mg}^{-1}$.

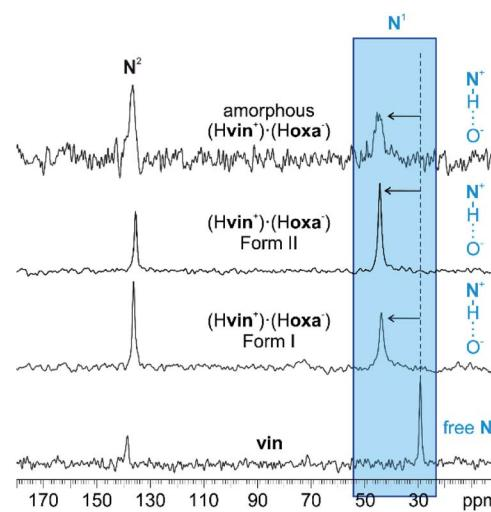


Fig. 2 ^{15}N CPMAS spectra of **vin**, crystalline $(\text{Hvin}^+) \cdot (\text{Hoxa}^-)$ forms I and II and amorphous $(\text{Hvin}^+) \cdot (\text{Hoxa}^-)$. The signal shifts, affiliated with the proton transfer from H_2oxa to **vin**, for the studied material are highlighted in blue. The ^{13}C spectra are shown in Fig. S34 in the ESI† document.



Experiments under LAG conditions, where liquid-additives were used in amounts greater than $\eta = 0.05 \mu\text{L mg}^{-1}$, resulted in three different outcomes. Based on these outcomes, we were able to classify the liquid additives in mechanochemical crystal screens of $(\text{Hvin}^+ \cdot \text{Hoxa}^-)$ as catalytic, inhibitive and prohibitive.

The first group of liquid additives, consisting of hexane, ethyl acetate, acetone and acetonitrile, enabled the formation of two crystalline $(\text{Hvin}^+ \cdot \text{Hoxa}^-)$ forms (see Fig. S1–S4 in the ESI† document). While hexane facilitated the formation of form I at $\eta = 0.15 \mu\text{L mg}^{-1}$ and $\eta = 0.30 \mu\text{L mg}^{-1}$, LAG experiments involving acetone, acetonitrile and ethyl acetate resulted in the formation of solvates, which swiftly undergo a complete desolvation at ambient conditions to yield a second polymorph of the salt (form II). Both crystal polymorphs were established as salts using ^{15}N CPMAS NMR spectroscopy and through the presence of the characteristic 44.3 ppm signal of the protonated $\text{N}^1(\text{vin})$ atom in the NMR spectra (Fig. 2). The formation of solvates was confirmed through thermal analyses, and in the case of the ethyl acetate solvate, also by single crystal X-ray diffraction studies. All liquid additives that enabled the formation of a crystalline $(\text{Hvin}^+ \cdot \text{Hoxa}^-)$ salt were described as *catalytic liquid additives* (Table 1).‡

The crystal structure of form I was determined using laboratory powder X-ray data. The salt crystallises in the $P2_1$ space group with one Hvin^+ cation and one Hoxa^- anion in the asymmetric unit. The Hoxa^- anions form helical molecular chains *via* C(5) O–H \cdots O $^-$ hydrogen bonds³⁰ (Fig. 3a). The helical structures are left-handed and exhibit a 7.6 Å pitch. The Hvin^+ cations link to the helical tapes *via* D(2) N $^+$ –H \cdots O $^-$ hydrogen bonds³⁰ (Fig. 3a and b). The $\text{Hvin}^+ \cdot \text{Hoxa}^-$ assemblies interact with each other through C–H \cdots O forces.

Form II was structurally characterised by single crystal X-ray diffraction using a crystal of an ethyl acetate salt hemisolvate, which was grown *via* slow solvent evaporation from an ethyl acetate solution and then spontaneously, rapidly and completely desolvated at ambient conditions in a single-crystal-to-single-crystal fashion.³¹ Structural analyses showed that the polymorph crystallises in the chiral space group $C2$; again, with one Hvin^+ cation and one Hoxa^- anion in the asymmetric unit.

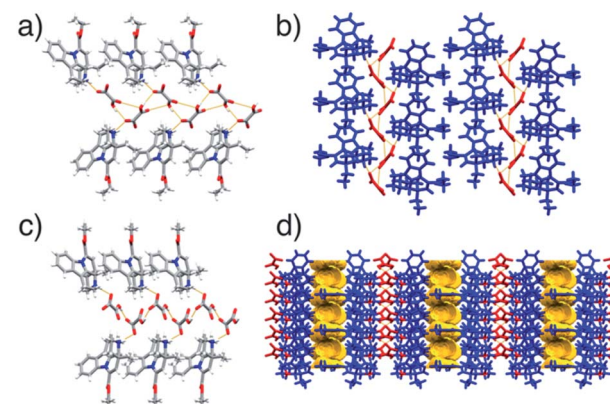


Fig. 3 Helical hydrogen-bonded $\text{Hvin}^+ \cdot \text{Hoxa}^-$ assemblies in the crystal structures of: (a) form I, viewed along the crystallographic planes (401) and (010); (b) form I, viewed along the crystallographic axis c. Crystal packing diagrams of $\text{Hvin}^+ \cdot \text{Hoxa}^-$ assemblies in: (c) form II, viewed along the crystallographic planes (103) and (010); and (d) form II, featuring voids (highlighted in yellow) and viewed along the crystallographic axis a.

The structure also features helical Hoxa^- chains that are, similarly to those seen in form I, sustained by C(5) O–H \cdots O $^-$ hydrogen bonds³⁰ and that interact with Hvin^+ cations *via* D(2) N $^+$ –H \cdots O $^-$ hydrogen bonds.³⁰ The pitch of the helical chain is, however, somewhat shorter and only 6.3 Å long (Fig. 3c). The helical assemblies interact with each other with a set of C–H \cdots O interactions that is different to that observed in form I. Notably, the crystal structure of form II exhibits sizeable voids ($V_{\text{void}} = 105 \text{ \AA}^3$ at 150 K), which are aligned along the crystallographic planes (110) and (002) (Fig. 3d). Details pertaining to the structural characterisation of forms I, II and the ethyl acetate hemisolvate are described in the ESI document (Fig. S32–S33 and Tables S1–S2†).

The relative stability of the two polymorphs was evaluated using periodic DFT-d methods and the CASTEP plane-wave code.³² The crystal structures were optimised using the Perdew–Burke–Ernzerhof (PBE) functional,³³ combined with the many-body dispersion (MBD*) correction.³⁴ The calculations revealed that form II is 14.3 kJ mol $^{-1}$ more stable than form I.

Table 1 Summary of liquid-assisted and neat grinding experiments performed with liquid additives that vary in their chemical nature (protic vs. aprotic), polarity (ϵ) and quantities used (η)^a

Liquid additive	Protic vs. aprotic	ϵ	$\eta/\mu\text{L mg}^{-1}$			Type of liquid additive	
			0.05	0.15	0.30		
Hexane	Aprotic	1.89	■	□	○ △	△	Catalytic
Ethyl acetate	Aprotic	6.02	■	■	▲	▲	
Acetone	Aprotic	20.7	■	■	▲	▲	
Acetonitrile	Aprotic	37.5	■	■	▲	▲	
Ethanol	Protic	24.5	■	■	■	■	Inhibitive
Methanol	Protic	32.7	■	■	■	■	
2-Pyrrolidone	Protic	23.6	■	○	○	○	
Nitromethane	Aprotic	35.9	■	○	○	○	
DMSO	Aprotic	47.2	■	○	○	○	Prohibitive

^a Amorphous salt: ■, physical mixture of reactants: ○, form I: △, form II: ▲.



Such relative stabilities are unexpected considering the higher density of form I, as compared to that of form II, but not unusual bearing in mind that the majority of cocrystals pack less efficiently in the crystalline state than their constituents.³⁵ We note that forms I, II and amorphous $(\text{Hvin}^+ \cdot (\text{H}_2\text{oxa}^-))$ show similar *in vitro* dissolution profiles, despite their significant structural differences (Fig. S35–S37 in the ESI† document).

The second group of liquids consists of ethanol and methanol. Both liquids enabled the formation of an amorphous salt, but not the formation of a crystalline product under LAG conditions at η values higher than $0.05 \mu\text{L mg}^{-1}$ (Fig. 1 and S5–S6 in the ESI† document). Since the additives appeared to curb or slow down the crystallisation of the product, they are described as *inhibitive liquid additives* (Table 1).

Lastly, the use of a third group of liquids, involving 2-pyrrolidone, dimethyl sulfoxide and nitromethane, unexpectedly yielded only physical mixtures of the reactants upon milling for 60 min at higher η values (0.15 and $0.30 \mu\text{L mg}^{-1}$) (Fig. 1 and S7–S9 in the ESI† document). This group of liquids appeared to preclude any chemical or physical reactivity and was accordingly categorised as *prohibitive liquid additives* (Table 1).

The prohibitive action of these three liquids clearly demonstrates that, in general, the role of liquid additives is significantly more complex than being solely a lubricant that facilitates molecular diffusion between colliding particles,³⁶ or a means to lower an energy pathway to the nucleation of a crystal form.³⁷ The initially observed prohibiting action of these additives raises the obvious question of whether they are indeed prohibiting the formation of a salt, or whether they are only severely delaying the transformation of a physical mixture of reactants into a crystalline salt through a transient amorphous salt phase.

To further test the prohibitive nature of this class of additives, we performed LAG experiments that involved the milling of the amorphous and crystalline salt forms with each of the prohibitive additives (namely nitromethane, DMSO and 2-pyrrolidone) for 60 min. Remarkably, the experiments revealed the disintegration of the salt into a physical mixture of the reactants when DMSO was used as additive (Table 2), thus proving that this liquid is indeed prohibiting the formation of the target solid. Such disintegration was not observed in LAG experiments involving nitromethane or 2-pyrrolidone. This observation is particularly interesting in light of the fact that forms I and II could not be converted into a physical mixture of crystalline **vin** and **H₂oxa** in the absence of liquid additives. Instead, the crystalline $(\text{Hvin}^+ \cdot (\text{H}_2\text{oxa}^-))$ salt was transformed into an amorphous salt when ground for 60 min without additives. The amorphous product was subsequently converted into crystalline forms I and II without difficulty using catalytic additives ethyl acetate and hexane (respectively), thereby emphasising the diversity of roles that liquid additives can play in mechanochemical crystal-form screens (Fig. 4 and S10–S12 in the ESI† document).

Further studies were focused on the role of water as inhibitor of the mechanochemical salt formation. Specifically, we aimed to elucidate whether atmospheric water suppresses the mechanochemical reactivity of **vin**:**H₂oxa** physical mixtures through the formation of viscous and thus unreactive solids, as previously observed by Tumanov *et al.*²³ These studies were prompted by the

Table 2 Summary of the outcomes of liquid-assisted grinding experiments involving multi-component crystals in the presence of prohibitive liquid additives^a

Crystal form	Structural changes		
	Nitromethane	DMSO	2-Pyrrolidone
$(\text{Hvin}^+ \cdot (\text{H}_2\text{oxa}^-))$, form I	△	○	■
$(\text{Hvin}^+ \cdot (\text{H}_2\text{oxa}^-))$, form II	■	○	■
(thp)·(23diFBA)	○	○	○
(thp)·(26diFBA)	■	○	●
2(thp)·3(ana)	■	○	●
(ibu)·(nic)	■	■	■
(pca)·(oxa)	○	●	●
(caf)·(cou)	■	■	■

^a No structural change observed: ■, partial or full decomposition into physical mixture of reactants: ○, partial or full decomposition into physical a mixture of a reactant and a new crystal form: ●, polymorphic transformation: △.

inevitable introduction of water into **vin**:**H₂oxa** reaction mixtures owing to the hygroscopic nature of anhydrous **H₂oxa** and its fast conversion into its hydrated form. Mechanochemical experiments involving water as additive have revealed the formation of a hydrated $(\text{Hvin}^+ \cdot (\text{H}_2\text{oxa}^-))$ salt, as evidenced by powder diffraction and thermogravimetric analysis. This demonstrates that the presence of atmospheric water (and water included in the crystals of **H₂oxa**) does not inhibit or prohibit mechanochemical reactions between **vin** and **H₂oxa** in any of the discussed experiments (see Fig. S25–S31 in the ESI† document).

In an effort to understand the observed effects of the selected liquid additives on the mechanochemical formation of $(\text{Hvin}^+ \cdot (\text{H}_2\text{oxa}^-))$, and to identify how various solvents affect its nucleation behaviour, we employed simple and accessible DFT-d calculations to study proton transfers from **H₂oxa** to **vin**,

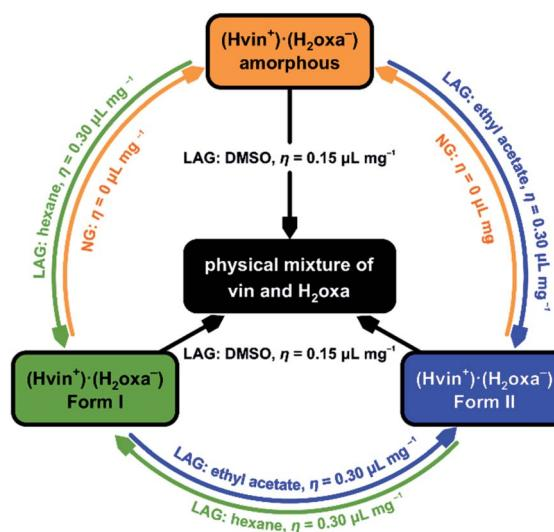


Fig. 4 Diagram summarising all interconversion LAG experiments performed and highlighting the catalytic, inhibitive and prohibitive actions of the studied liquid additives.



and the stability of $\text{Hvin}^+ \cdot \text{Hoxa}^-$ assemblies in a range of solvent environments, which were represented using a continuum SMD model (see Table S3 in the ESI† document for computational results and a brief discussion thereof).³⁸ The inability to rationalise the prohibitive, inhibitive and catalytic actions of the studied additives on the crystallisation of forms I and II using such basic DFT-d methods suggests that more elaborate computational methods need to be employed. We envision that a fundamental understanding of the described phenomena will be likely reached through the combined use of large-scale molecular dynamics simulations and DFT-d calculations. We note that molecular dynamics simulations were recently successfully employed by Ferguson *et al.* to simulate the early stages of mechanochemical cocrystallisations and to study the effects of small amounts of liquid additives on mechanochemical cocrystal formation,³⁷ while DFT-d calculations were utilised by Belenguer *et al.* to evaluate solvation and surface effects on the stabilities of mechanochemically prepared polymorphs of organic compounds.³⁹

The prohibitive action of liquid additives described herein is not an isolated case, as evidenced by other instances where the addition of a particular liquid to a solid reaction mixture precluded the formation of a cocrystal. For example, one such instance was recently discovered in our laboratories during an unrelated study of supramolecular synthons in a series of cocrystals composed of theophylline and fluorobenzoic acid isomers.⁴⁰ The cocrystallisation of theophylline (**thp**) with the fluorobenzoic acids was attempted through LAG and it was found that a cocrystal cannot be prepared using 2,3- and 2,6-difluorobenzoic acid (**23diFBA** and **26diFBA**, respectively) as cocrystal formers when nitromethane is used as liquid additive. While the cocrystallisation of the elusive cocrystals was readily achieved using ethanol as additive (Fig. S23–S24 in the ESI† document), the fact that nitromethane prohibited the formation of $(\text{Hvin}^+) \cdot (\text{Hoxa}^-)$ and the two theophylline cocrystals raised the question of whether its prohibitive action is specific only to the three studied solids, or whether nitromethane (as well as 2-pyrrolidone and DMSO) can be more generally regarded as prohibitive. Our curiosity was further heightened by a serendipitous discovery during an attempt to prepare form I of the $(\text{Hvin}^+) \cdot (\text{Hoxa}^-)$ salt. Specifically, we found that the inadvertent use of cyclohexane, instead of hexane, prevented the formation of the salt. This recalled the fact that cyclohexane precluded the formation of three different cocrystals in studies reported by Friščić, Childs, Rizvi and Jones.^{17,18} With these examples in mind, we subjected the two **thp** cocrystals and another four arbitrarily selected cocrystals (which are based on **thp**, H_2oxa , ibuprofen (**ibu**), paracetamol (**pca**), caffeine (**caf**), nicotinamide (**nic**), anthranilic acid (**ana**)) to LAG in the presence of the prohibitive additives. We found a substantial number of cases in which the use of a prohibitive additive led to the decomposition of the cocrystal into a physical mixture of its constituents (Table 2 and Fig. S38–S57 in the ESI† document). The mechanistic aspects of the observed cocrystal disintegration are, so far, not understood. But keeping in mind that nitromethane, for example, is commonly and successfully used in cocrystal screens,⁴⁰ we reason that the prohibitive action of

a liquid additive is specific to certain multi-component crystal systems, rather than general and applicable to a larger group of cocrystal systems.

Conclusions

We have shown that mechanochemical reactivity can be inhibited, prohibited and reversed with the use of liquid additives. Our findings, and attempts to rationalise them, stress the current gaps in our knowledge about the role of liquid additives in mechanochemical reactions, as well as the urgent need to study and understand solvent effects in mechanochemical reactions. Our discoveries also suggest that widely accepted and commonly utilised procedures for mechanochemical crystal-form screens (wherein the use of only one solvent as liquid additive is deemed as suitable), should be revised. Specifically, we recommend the use of numerous types of liquid additives in crystal form screens in order to eliminate the possible occurrence of false negative results, which can seriously obstruct the development of marketable functional materials in industrial research and development exercises. We also speculate that liquid additives may be able to act prohibitively in other mechanochemical processes relevant to chemical and materials synthesis.^{41,42} We are therefore engaging in further studies to elucidate the mechanisms through which the reported solid-state reactions are catalysed, inhibited and prohibited. These will also include investigations into the role of (un)intentional seeding on the action of the different additive types.^{43,44}

Conflicts of interest

There are no conflicts of interest to declare.

Acknowledgements

M.A. thanks the National Science Center of Poland for the financial support *via* SONATA grant (2018/31/D/ST5/03619). Periodic and molecular DFT calculations were performed on the *Prometheus* supercomputer (*Cyfronet*, Krakow) to which access was granted *via* the PLGrid consortium. The UK's EPSRC is acknowledged for the funding of the crystallographic studies *via* grant EP/K03930X/1. Divya Amin is gratefully acknowledged for her help with the collection of capillary powder X-ray diffraction data. Prof. Gareth R. Williams, Sebastian Gurgul and Karolina Dziemidowicz are thanked for their help with TGA and DSC measurements. Professor Krzysztof Woźniak is gratefully acknowledged for access to the TGA/DSC instrument and Professor Damian Pociecha for assisting with powder X-ray diffraction experiments performed at the University of Warsaw. The Reviewers are thanked for useful discussions and suggestions.

Notes and references

‡ We note that ethyl acetate, acetonitrile and acetone may be also suitably described as *reactants* in the mechanochemical formation of the hemisolvate of the $(\text{Hvin}^+) \cdot (\text{Hoxa}^-)$ salt. But considering that these liquids also template the formation of solvent-free and porous form II, we find that they are well suited to be described as *catalytic liquid additives*.



Open Access Article. Published on 20 January 2021. Downloaded on 2/9/2026 1:34:27 PM.
This article is licensed under a Creative Commons Attribution-NonCommercial 3.0 Unported Licence.

1 S. Aitipamula, R. Banerjee, A. K. Bansal, K. Biradha, M. L. Cheney, A. R. Choudhury, G. R. Desiraju, A. G. Dikundwar, R. Dubey, N. Duggirala, P. P. Ghogale, S. Ghosh, P. K. Goswami, N. R. Goud, R. R. K. R. Jetti, P. Karpinski, P. Kaushik, D. Kumar, V. Kumar, B. Moulton, A. Mukherjee, G. Mukherjee, A. S. Myerson, V. Puri, A. Ramanan, T. Rajamannar, C. M. Reddy, N. Rodriguez-Hornedo, R. D. Rogers, T. N. G. Row, P. Sanphui, N. Shan, G. Shete, A. Singh, C. C. Sun, J. A. Swift, R. Thaimattam, T. S. Thakur, R. Kumar Thaper, S. P. Thomas, S. Tothadi, V. R. Vangala, N. Variankaval, P. Vishweshwar, D. R. Weyna and M. J. Zaworotko, *Cryst. Growth Des.*, 2012, **12**, 2147–2152.

2 N. K. Duggirala, M. L. Perry, Ö. Almarsson and M. J. Zaworotko, *Chem. Commun.*, 2016, **52**, 640–655.

3 G. Bolla and A. Nangia, *Chem. Commun.*, 2016, **52**, 8342–8360.

4 K. Fucke, M. J. G. Peach, J. A. K. Howard and J. W. Steed, *Chem. Commun.*, 2012, **48**, 9822–9824.

5 B. Sandhu, A. S. Sinha, J. Desper and C. B. Aakeröy, *Chem. Commun.*, 2018, **54**, 4657–4660.

6 L. Casali, L. Mazzei, O. Shemchuk, L. Sharma, K. Honer, F. Grepioni, S. Ciurli, D. Braga and J. Baltrusaitis, *ACS Sustainable Chem. Eng.*, 2019, **7**, 2852–2859.

7 H. Jiang and W. Hu, *Angew. Chem., Int. Ed.*, 2019, **59**, 1408–1428.

8 H. M. Titi, M. Arhangelskis, G. P. Rachiero, T. Friščić and R. D. Rogers, *Angew. Chem., Int. Ed.*, 2019, **131**, 18570–18575.

9 C. B. Aakeröy, T. K. Wijethunga and J. Desper, *Chem.-Eur. J.*, 2015, **21**, 11029–11037.

10 K. B. Landenberger, O. Bolton and A. J. Matzger, *J. Am. Chem. Soc.*, 2015, **137**, 5074–5079.

11 D.-K. Bučar, S. Filip, M. Arhangelskis, G. O. Lloyd and W. Jones, *CrystEngComm*, 2013, **15**, 6289–6291.

12 A. V. Trask, *Mol. Pharm.*, 2007, **4**, 301–309.

13 Ö. Almarsson, M. L. Peterson and M. Zaworotko, *Pharm. Pat. Anal.*, 2012, **1**, 313–327.

14 K. Fucke, S. A. Myz, T. P. Shakhtshneider, E. V. Boldyreva and U. J. Griesser, *New J. Chem.*, 2012, **36**, 1969–1977.

15 S. L. James, C. J. Adams, C. Bolm, D. Braga, P. Collier, T. Friščić, F. Grepioni, K. D. M. Harris, G. Hyett, W. Jones, A. Krebs, J. Mack, L. Maini, A. G. Orpen, I. P. Parkin, W. C. Shearouse, J. W. Steed and D. C. Waddell, *Chem. Soc. Rev.*, 2012, **41**, 413–447.

16 D. Hasa and W. Jones, *Adv. Drug Delivery Rev.*, 2017, **117**, 147–161.

17 T. Friščić, S. L. Childs, S. A. A. Rizvi and W. Jones, *CrystEngComm*, 2009, **11**, 418–426.

18 N. Shan, F. Toda and W. Jones, *Chem. Commun.*, 2002, 2372–2373, DOI: 10.1039/B207369M.

19 K. Lien Nguyen, T. Friščić, G. M. Day, L. F. Gladden and W. Jones, *Nat. Mater.*, 2007, **6**, 206–209.

20 A. V. Trask, N. Shan, W. D. S. Motherwell, W. Jones, S. Feng, R. B. H. Tan and K. J. Carpenter, *Chem. Commun.*, 2005, 880–882, DOI: 10.1039/B416980H.

21 D. Braga, S. L. Giaffreda, F. Grepioni, M. R. Chierotti, R. Gobetto, G. Palladino and M. Polito, *CrystEngComm*, 2007, **9**, 879–881.

22 E. Boldyreva, *Chem. Soc. Rev.*, 2013, **42**, 7719–7738.

23 I. A. Tumanov, A. A. L. Michalchuk, A. A. Politov, E. V. Boldyreva and V. V. Boldyreva, *Dokl. Chem.*, 2017, **472**, 17–19.

24 D. Hasa, D. Voinovich, B. Perissutti, M. Grassi, A. Bonifacio, V. Sergo, C. Cepek, M. R. Chierotti, R. Gobetto, S. Dall'Acqua and S. Invernizzi, *Pharm. Res.*, 2011, **28**, 1870–1883.

25 Y. Zhang, J.-d. Li and C. Yan, *Eur. J. Pharmacol.*, 2017, 819.

26 A. J. Cruz-Cabeza, *CrystEngComm*, 2012, **14**, 6362–6365.

27 M. K. Corpinot and D.-K. Bučar, *Cryst. Growth Des.*, 2019, **19**, 1426–1453.

28 D. Hasa, E. Miniussi and W. Jones, *Cryst. Growth Des.*, 2016, **16**, 4582–4588.

29 P. Cerreia Vioglio, M. R. Chierotti and R. Gobetto, *Adv. Drug Delivery Rev.*, 2017, **117**, 86–110.

30 M. C. Etter, J. C. MacDonald and J. Bernstein, *Acta Crystallogr., Sect. B: Struct. Crystallogr. Cryst. Chem.*, 1990, **46**, 256–262.

31 A. J. Cruz Cabeza, G. M. Day, W. D. S. Motherwell and W. Jones, *Chem. Commun.*, 2007, 1600–1602, DOI: 10.1039/B701299C.

32 S. J. Clark, M. D. Segal, C. J. Pickard, P. J. Hasnip, M. I. J. Probert, K. Refson and M. C. PayneII, *Z. Kristallogr.*, 2005, **220**, 567–570.

33 J. P. Perdew, K. Burke and M. Ernzerhof, *Phys. Rev. Lett.*, 1996, **77**, 3865–3868.

34 A. Tkatchenko, R. A. DiStasio, R. Car and M. Scheffler, *Phys. Rev. Lett.*, 2012, **108**, 236402.

35 C. R. Taylor and G. M. Day, *Cryst. Growth Des.*, 2018, **18**, 892–904.

36 T. Friščić and W. Jones, *Cryst. Growth Des.*, 2009, **9**, 1621–1637.

37 M. Ferguson, M. S. Moyano, G. A. Tribello, D. E. Crawford, E. M. Bringa, S. L. James, J. Kohanoff and M. G. Del Pópolo, *Chem. Sci.*, 2019, **10**, 2924–2929.

38 A. V. Marenich, C. J. Cramer and D. G. Truhlar, *J. Phys. Chem. B*, 2009, **113**, 6378–6396.

39 A. M. Belenguer, G. I. Lampronti, A. J. Cruz-Cabeza, C. A. Hunter and J. K. M. Sanders, *Chem. Sci.*, 2016, **7**, 6617–6627.

40 M. K. Corpinot, S. A. Stratford, M. Arhangelskis, J. Anka-Lufford, I. Halasz, N. Judaš, W. Jones and D.-K. Bučar, *CrystEngComm*, 2016, **18**, 5434–5439.

41 J. L. Howard, Q. Cao and D. L. Browne, *Chem. Sci.*, 2018, **9**, 3080–3094.

42 T. Friščić, C. Mottillo and H. M. Titi, *Angew. Chem., Int. Ed.*, 2020, **59**, 1018–1029.

43 D.-K. Bučar, G. M. Day, I. Halasz, G. G. Z. Zhang, J. R. G. Sander, D. G. Reid, L. R. MacGillivray, M. J. Duer and W. Jones, *Chem. Sci.*, 2013, **4**, 4417–4425.

44 D. Hasa, M. Marosa, D.-K. Bučar, M. K. Corpinot, D. Amin, B. Patel and W. Jones, *Cryst. Growth Des.*, 2020, **20**, 1119–1129.